FWI with source illumination: A synthetic case study

Babatunde Arenrin, Gary Margrave, and John Bancroft

ABSTRACT

We study incorporating well log information into Full Waveform Inversion (FWI) and compare the result with a line search optimization scheme. We test this approach using a poor starting model i.e. a linear velocity v(z) model and also using smoothed version of the true velocity model. Our results show that incorporating well information into FWI saves a lot of computational time compared with a line search optimization scheme. Although the inverted model is far from convergence, we learn a few interesting things: conventional FWI cannot by itself provide good estimate for layer properties when the starting model is poor such as the case of a linear v(z) model, the information from well logs can be used to constrain the line search calculation and still save computational time, finally low frequencies are crucial for convergence.

INTRODUCTION

Full waveform inversion is an optimization technique that seeks to find a model of the subsurface that best matches the recorded field data at every receiver location. The method begins from a best guess of the true model, which is iteratively improved using linearized inversions methods although the FWI problem is non-linear (Warner et al, 2013). FWI is formulated as a generalised inverse problem with a numerical solver-a forward modelling code and its adjoint. FWI can be viewed as an iterative cycle involving modelling, pre-stack migration and velocity model updating in each iteration (Margrave et al, 2010).

Despite its success, FWI suffers from cycle skipping problems, and convergence problems when the starting model is far from the true model and in the absence of low frequencies. However different approaches have been developed to mitigate the problems with conventional FWI, such as incorporating well information to FWI (Margrave et al, 2011a). Well information can aid in (1) calculating the step-length (a scalar which multiplies the gradient for the model update), (2) constraining the line search calculation used in a steepest descent optimization scheme, and (3) improving the wavelet estimate which is essential for proper updates. Some other approaches that mitigate the problems with conventional FWI are Tomographic Full waveform Inversion (TFWI) which combines both FWI and WEMVA (Biondi and Almomin,2012), and Adaptive Waveform Inversion (AWI) in which the observed and predicted datasets are matched trace-by-trace using a least squares convolutional filter (Warner and Guasch, 2014).

In this paper, we test conventional FWI using a linear velocity v(z) model and a smooth version of the true model as our starting model, for the case of three-flat layers. For the optimization scheme, we test using a line search method and calculating an update using information from well logs.

For the case of geological structures, we use a smooth velocity model as the starting model, and for the optimization scheme, we compare the result using a line search method and calculating an update using information from well logs.

THEORY AND METHOD

The theory of FWI has been described in literature by Tarantola (1984), Lailly (1983). Pratt et al, (1998) used a frequency-space modelling formalism for FWI. A full mathematical derivation of the theory of FWI can be found in these papers. FWI compares observed and predicted data by subtracting the two datasets to obtain a residual, for real data we anticipate that this residual should be minimized in a least square sense. The FWI objective function is the L_2 norm of the residuals and can be represented mathematically as

$$\phi_k = \sum_{s,r} \left(\psi - \psi_k\right)^2 , \tag{1}$$

where ϕ_k is the objective function we want to minimize, s,r are the sources and receivers over which the sum is taken, ψ is the observed data, and ψ_k is the predicted data for the k^{th} iteration (Margrave et al, 2010).

If we are interested in inverting for the velocity model of the subsurface, the model update can be expressed as the gradient of the objective function multiplied by a scalar expressed mathematically as

$$\delta v_k(x,z) = \lambda \int \sum_{s,r} \omega^2 \hat{\psi}_s(x,z,\omega)\delta\hat{\psi}^*_{r(s),k}(x,z,\omega)d\omega \tag{2}$$

where λ is a scalar, the hat (^) over a variable indicates its temporal Fourier transform, $\hat{\psi}_s\left(x,z,\omega\right)$ is a model of the source wavefield for source s propagated to all $\left(x,z\right)$, ω is temporal frequency, $\delta\hat{\psi}_{r(s),k}\left(x,z,\omega\right)$ is the kth data residual for source s back propagated to all $\left(x,z\right)$, and $*$ is complex conjugation. Specifically $\delta\hat{\psi}_{r(s),k}\left(x,z,\omega\right) = \hat{\psi}_{r(s)}\left(x,z,\omega\right) - \hat{\psi}_{r(s),k}\left(x,z,\omega\right)$ where $\hat{\psi}_{r(s)}\left(x,z,\omega\right)$ is the real data at receivers $r\left(s\right)$ as back propagated into the medium and $\hat{\psi}_{r(s),k}\left(x,z,\omega\right)$ is the kth data model for the same. (Margrave et al, 2010).

The calculation of the scalar λ in Equation 1 is one-part of the focus of this paper. The scalar can be calculated using a line search algorithm to calibrate the migrated image into a model update. This is the steepest descent optimization scheme.

However, if we have well control, we can calculate a scalar that compares the current velocity model to that of the known velocity at the well location. We now define an objective function β which is the L2 norm of the difference between the model update calculated from migrating the data residuals and the known velocity at the well and the background velocity model expressed by,

$$\beta = \left\| \lambda G_k - \left(V_{well} - V_{BG} \right)_k \right\|^2 \tag{3}$$

where G_k is the migration of the data residuals stacked over all shots at the well location, V_{well} is the known velocity at the well location, V_{BG} is the background velocity (or the migration velocity) at the well location, and the L2 norm is taken over all the samples in the well. (With real data it is necessary to resample the well information to the same sample density as the velocity model).

The scalar λ we wish to find is calculated by minimizing the objective function β in Equation 3 with respect to λ, and making λ the subject of the expression, this gives

$$\lambda = \frac{\sum_j \delta V_j G_j}{\sum_j G_j^{\,2}} \tag{4}$$

where $\delta V_j = \left(V_{well} - V_{BG} \right)_j$ and j indicates sample number.

We test the two methods of calculating λ discussed above to flat layers, and layers with structures. In the case of the flat layers, we also test two types of starting models: a very smooth version of the true velocity model, and a linear velocity v(z) model. It turns out that we learn a few interesting things from the flat layer geology and we will discuss our findings in subsequent sections.

Forward modelling and migration (inversion)

For the flat layer velocity model and the velocity model with structures, we use an acoustic finite-difference forward-modelling code to generate the shot records, and we generate 40 shots in each case. The shot spacing is 50 meters, receiver spacing is 5 meters and 448 receivers. The source wavelet is minimum wavelet with a dominant frequency of 50 hertz. All boundaries are absorbing except at the ground-air interface.

For the migration of the data residuals, we use a phase shift plus interpolation (PSPI) algorithm (Gazdag and Squazerro, 1984). The PSPI algorithm outputs a cross correlation Imaging Condition (IC) reflectivity image, a deconvolution IC image, and a source illumination. Margrave et al, in their papers (2010, and 2011a) show a mathematical formulation of the deconvolution IC. In this paper we use the deconvolution IC output from PSPI for the gradient calculation. One advantage of using PSPI is that it works in the frequency domain, therefore we did not apply a bandpass filter to the data residuals before migration when implementing a multi-scale FWI approach (the multi-scale approach means starting the the inversion with low frequencies and moving to higher frequencies) as suggested by Pratt (Pratt,1999).

EXAMPLES

In this section we will treat the case of the flat layer model and the case of the model with structures separately. In Case 1(a and b), we will discuss our findings using a flat layer model (1D model). In Case 2 we will discuss our findings using a structured model (2D model). Finally, we will discuss the results from the flat layer model and the model with structures.

Case 1-a: Comparing inverted velocity model using linear velocity v(z) as starting model with the inverted velocity model using a smooth version of the true model.

In this case we present the results using a linear velocity v(z) model and a smooth version of the true model as the starting model for FWI. The true model consists of three layers with velocities 2.5Km/s, 3Km/s and 3.5Km/s. A steepest descent optimization scheme is used for the inversion. We use a multi-scale approach as suggested by Pratt (1999).

Table 1 gives a summary of the frequency band used in the iterations for Case 1(a and b). Figure 1 is the result of using a smooth velocity model and a linear velocity v(z) model as the staring model.

After 50 iterations, the inverted model using a linear velocity model doesn't seem to be converging despite the fact that the inversion was giving a head start by replacing the gradient model from the surface down to about 310 meters with a smooth velocity profile close to the true velocity as shown in Figure 2. This is done so that the direct or first arrivals can be modelled correctly.

On the other hand, the smooth velocity seems to be converging. We stopped the inversion after 50 iterations for reasons that we will be discussing in later in this paper.

Iteration	Frequency band (hertz)
1-10	1-5
11-20	3-8
21-30	5-11
31-40	3-8
41-50	1-5

Table 1. Frequency bands for the iterations in Case 1.

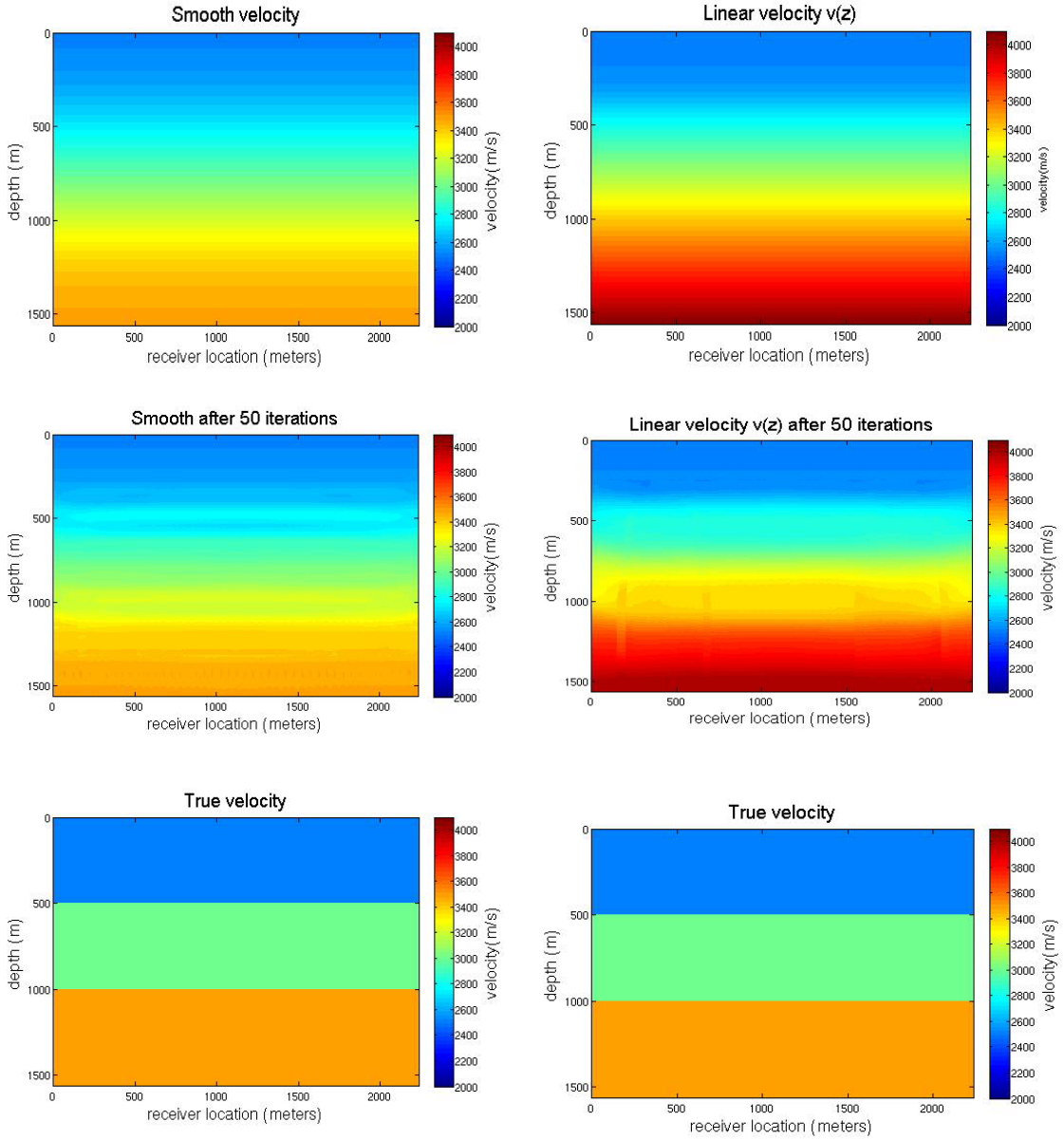

FIG 1. True model, starting models and inverted models after 50 iterations. Smooth version of the true model (top left), stating model with linear velocity v(z) (top right), inverted model using the smooth model as starting model (middle left), inverted model using the linear velocity v(z) model as staring model (middle right), true velocity model (bottom left and bottom right).

Figure 2 shows a vertical profile of the true, starting and inverted models at 520 meters receiver location. Figure 3 shows the true model and inverted models at the same location. We see that the inverted velocity models using the smooth version of the true model as starting model is approaching the true model. Although the inverted model is quite far from converging, it gives a better result than the inverted model using a linear velocity v(z) model.

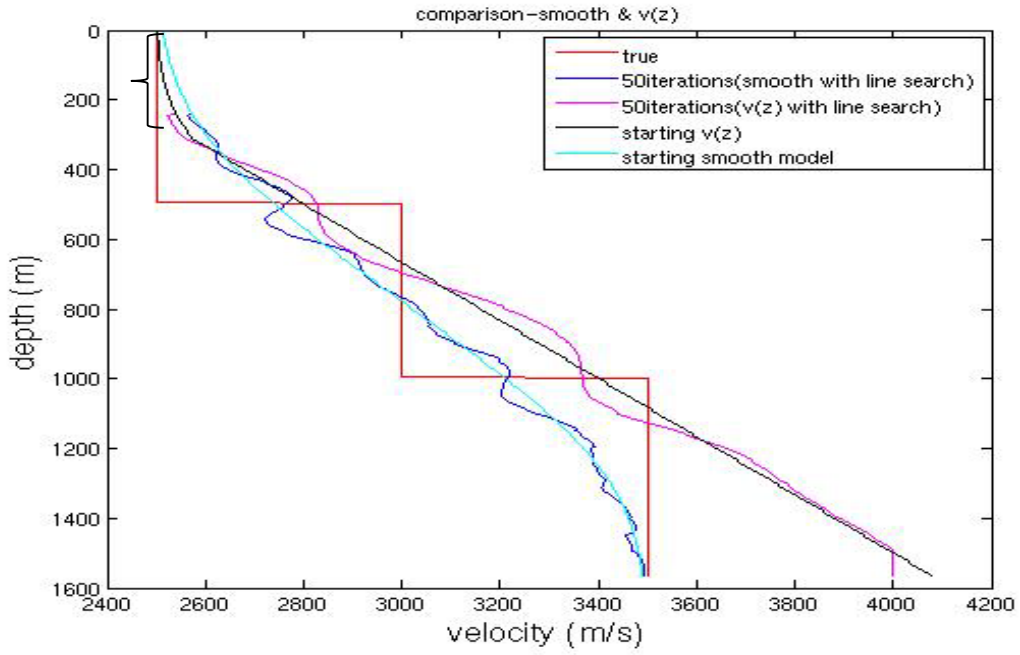

FIG 2. Comparison of the true velocity model (red), inverted model using a smooth version of the true model as starting model (blue), inverted model using a linear velocity v(z) as starting model(magenta), starting model linear velocity v(z) (black), starting model using a smooth version of the true model (cyan) at 520 meters receiver location. The segment where the linear velocity v(z) model was replaced with a smooth profile (curly brackets).

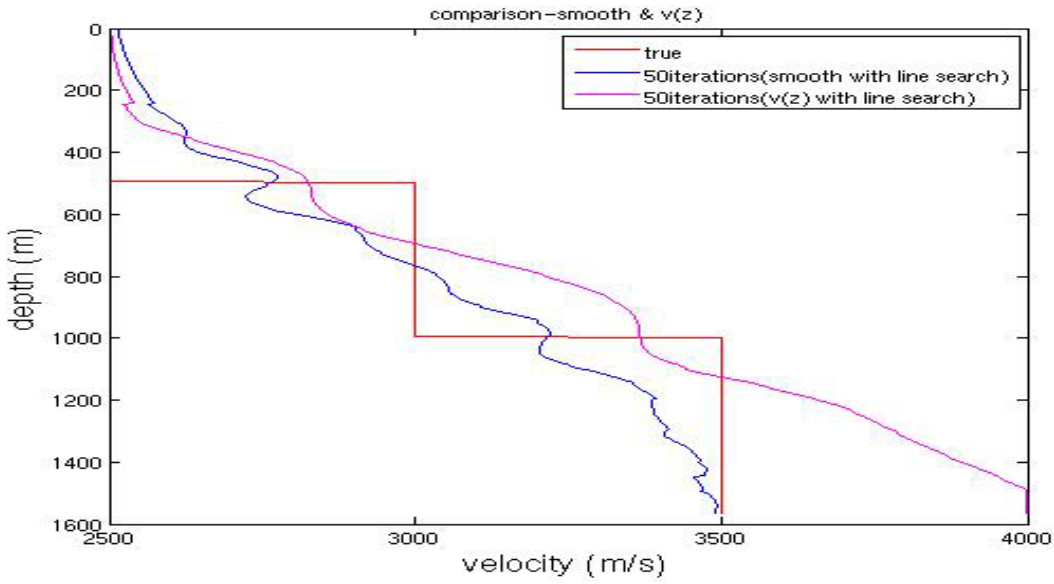

FIG 3. Comparison of the true velocity (red), inverted model using a smooth version of the true model as starting model (blue), inverted velocity model using a linear velocity v(z) as starting model(magenta) at 520 meters receiver location.

Case 1-b: Comparing inverted model from incorporating well information with inverted model using a line search. The starting velocity is a smooth version of the true model.

In this case we present the results using a smooth model of the true model as the starting model for FWI. The true model is the same as case 1-a, however we use different methods to calculate the scalar that converts the migrated data residuals to a velocity perturbation. The first method uses a line search algorithm, and other method uses a calibration process at the well and the scalar is calculated using Equation 4.

Figures 4 and 5 show the inverted models after 50 iterations. The inverted models look similar but a closer look at the vertical velocity profiles (Figure 4) reveals subtle differences. Looking at Figure 4 carefully, the updates using well information has done a better job in the cause of 50 iterations.

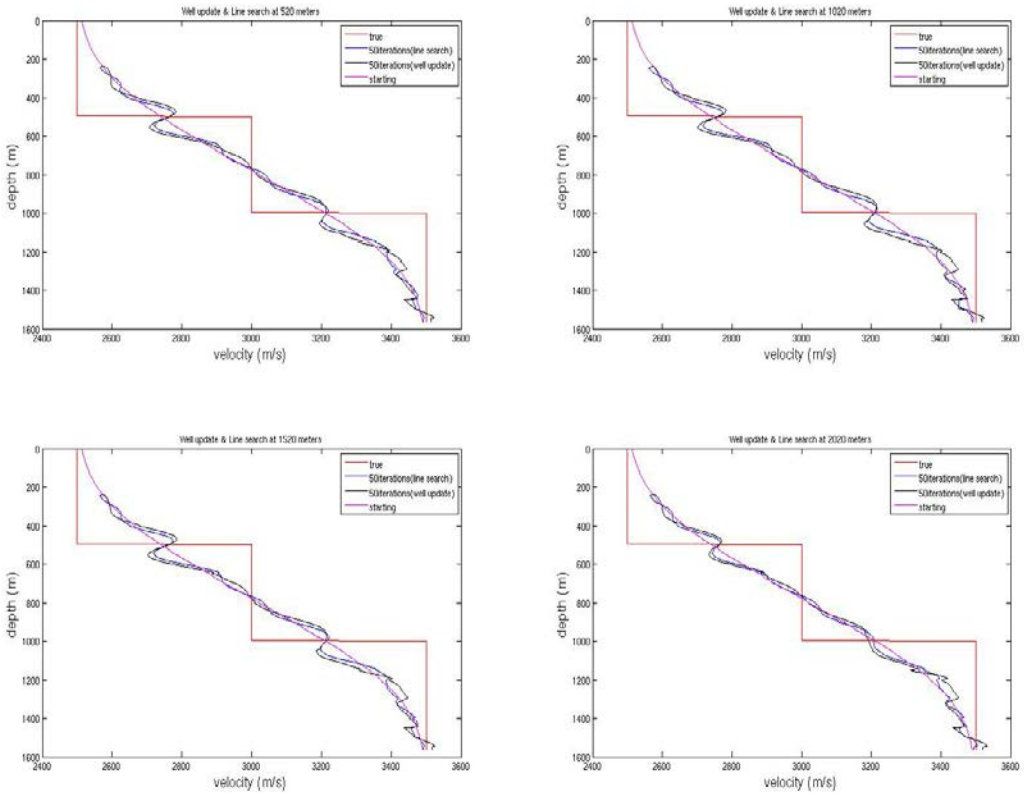

FIG 4. Vertical velocity profiles taken at four receiver locations. Velocity profiles at: 520 meters (top left),1020 meters (top right),1520 meters (bottom left) and 2020 meters (bottom right).True model (red), inverted model using line search (blue), inverted model using well information (black) and the starting model (magenta).

Figure 5 shows the final velocity models after 50 iterations for Case 1-b. The inverted model using well information (middle left) has resolved the bottom part of the model better than the inverted model using a line search. This is not surprising because we have well control at the bottom section of the model. However, the two approaches have done a reasonable job at the upper section of the model. The red lines on the models indicate the well location.

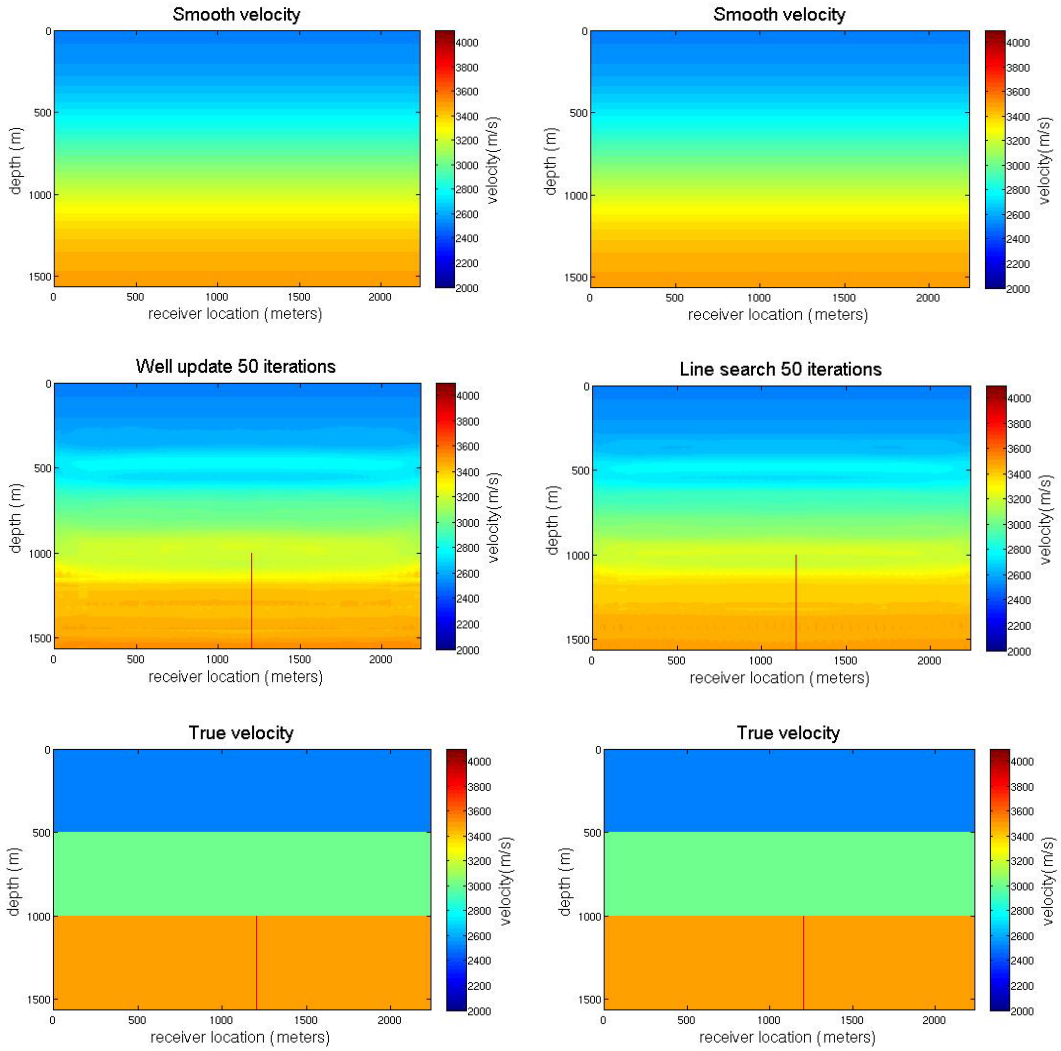

FIG 5. True model, starting model and inverted models after 50 iterations. Smooth velocity model (top left and top right), inverted velocity model using well information (middle left), inverted velocity model using a line search (middle right), true velocity model (bottom left and bottom right). The red lines indicate the well location.

Now we compare the path the two methods took to arrive at the inverted models above, and we will make some observations. Figure 6 below is a plot of the scalars calculated using Equation 4 and the scalars computed from a line search code. The scalar computed from the line search on the first iteration seems very anomalous so we choose to exclude it from our analysis as is done in Figure 7. We will base our observations on this plot.

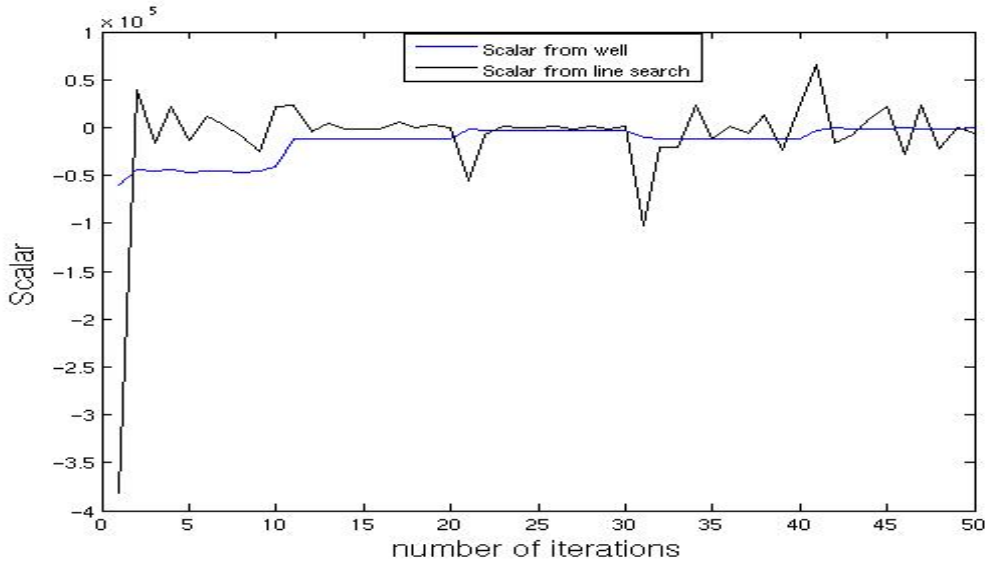

FIG 6. Plot of the scalar calculated using well information (blue), and computed using a line search code (black).

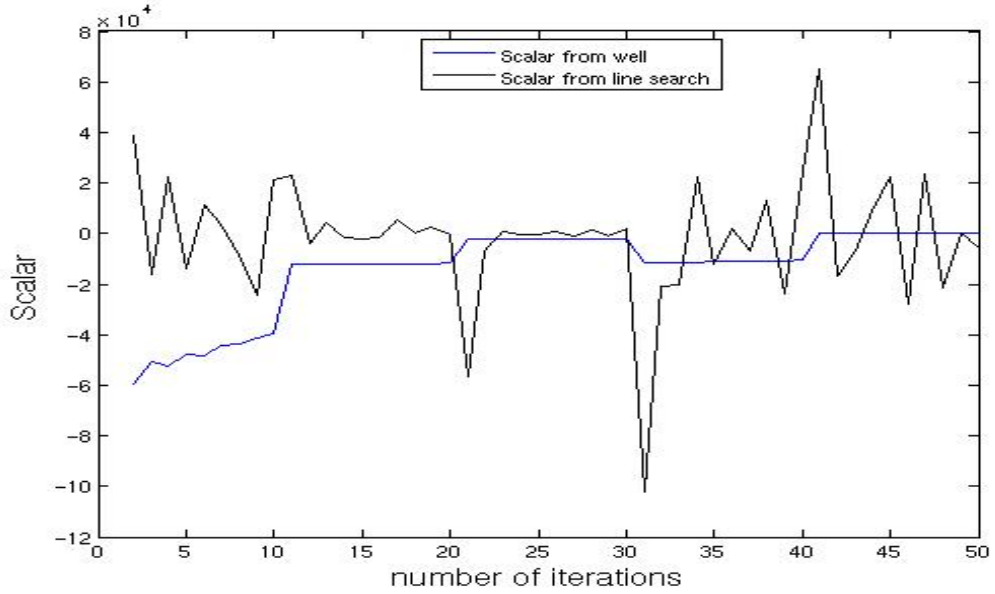

FIG 7. Plot of the scalar calculated using well information (blue), and computed using a line search code (black). The scalar from the 1st iteration has been ignored.

The plot in Figure 7 shows the calculated scalar using Equation 4 changes its pattern which coincides with a change in the frequency band during the iteration. However, the scalar from the line search shows greater fluctuations.

One would expect that solving an optimization problem, subsequent iterations should get us closer to the true solution assuming we are not heading for the local minimum. If this is true, then we would expect that the model update (and the scalar) should get progressively smaller with subsequent iterations. Based on this, we will argue that the

scalar calculated using well information seems to conform to what we expect. However, we cannot make conclusions based on this model as we will like to run tests with more realistic models.

Figure 8 is similar to Figure 7 except that we have plotted the negative of the scalar calculated using well information (red). Looking at Figure 8, the scalars calculated from the line search code appear to lie within the range of plus or minus the value of the scalars calculated using well information. Surely a few points lie outside this range, however we think it is possible to constrain the line search code to search for scalars in the region of plus or minus the calculated scalar using well information. This can save us computational time on the number of forward modelling operations that we would have to run if there is no well information.

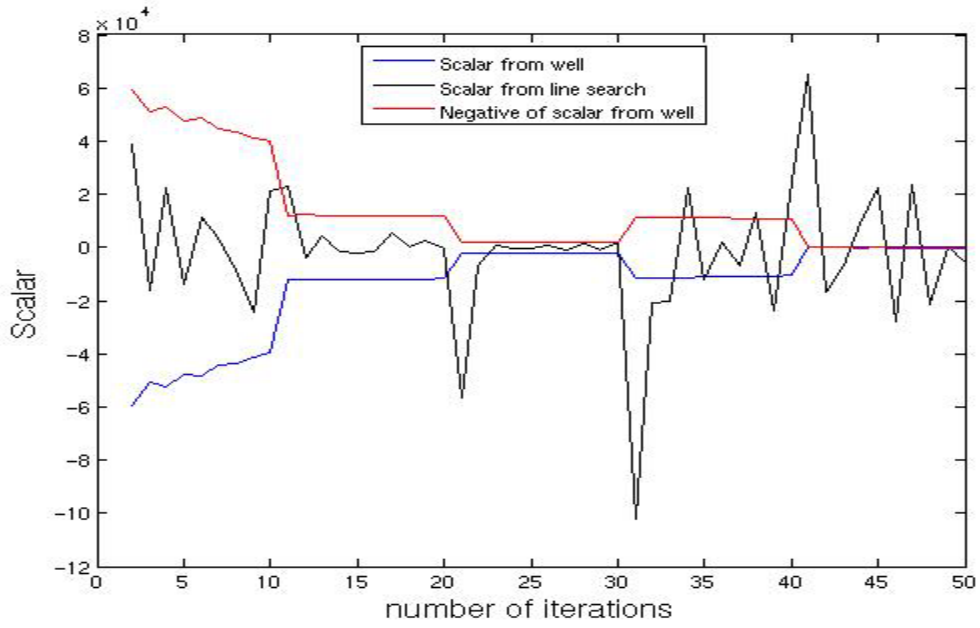

FIG 8. Plot of the scalar: calculated from well information (blue), from a line search code (black). The additive inverse of the scalar calculated from well information (red). The scalar from the 1st iteration has been ignored.

In Case 1 discussed above, we observe that the inverted models are not close to the true model, it may be possible that should we continue with the iteration, the model will converge to the true model, but we are not sure how many iterations this would take. At this juncture, we believe that the flat layer model is not realistic however, we will shed more light on our thoughts in the discussions section.

Case 2: Comparing inverted model by incorporating well information with inverted model using a line search of a structured model.

In Case 2 we present the results using different optimization schemes for FWI. The true model has a few dipping layers and an asymmetric intrusive structure surrounded by high velocity layers at the base of the model. We compare calculating a scalar for the

model update using Equation 4 with a line search optimization scheme. We also use a multi-scale approach suggested by Pratt (1999) in this case.

We use a very smooth version of the true model as the starting model. As we can see from Figure 9 below, the starting model contains no distinct reflectors between 300 and 1565 meters. The inverted velocity models 45 iterations from the two methods shown in Figure 9. We observe that the two methods are doing their best to obtain the correct model.

The inverted velocity model using well information seems to have done a better job between 500 and 1565 meters. Between these depths, we can see reflectors appearing. The sides of the intrusion at the base of the model can be mapped, and the reflectors above the intrusion can be interpreted. We find that the best inverted model using well information is obtained at the 45^{th} iteration. Beyond the 45^{th} iteration, the inverted model starts to blow up, therefore we stopped at the 45^{th} iteration. The scalar used to update the migrated residuals at each stage in the iteration process was calculated using Equation 4. The location of the well is at 1100 meters and it is represented as a black line on the models.

The well penetrates the side of the intrusion and extends from 1040 to 1565 meters. The well penetrates only 2 sedimentary layers before penetrating the side of the intrusion, therefore we can assume that we don't have good well coverage in the area. However, we are still able to get a reasonable inverted model using this well.

The inverted velocity using a line search optimization scheme appears to have done a better job than the inverted model using well information at the top of the model between 0 and 500 meters. The reflectors are quite visible and we can start to make interpretations on this model. The best inverted model we found using a line search optimization scheme was at the 90^{th} iteration.

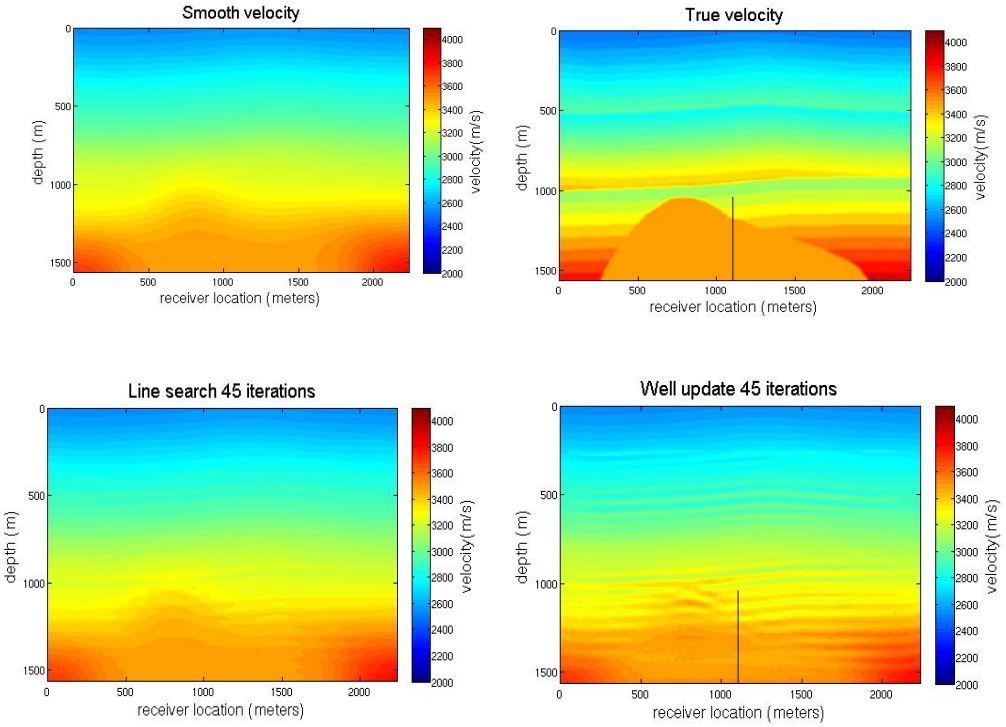

FIG 9. True model, starting model and inverted models after 45 iterations. Smooth velocity model (top left), true velocity model (top right). Inverted model after 45 iterations using a line search (bottom left), inverted model using well information (bottom right). The black lines indicate the well location (1100 meters).

Figure 10 is a plot of the vertical profile of the inverted velocity model after 45 iterations using well information at the well location (1100 meters). The vertical profile shows that the inverted model is close to the true model at depths between 500 and 800 meters, and at depths between 1200 and 1565 meters. The inverted model appears shifted in time between 200 and 400 meters.

Figure 11 is a plot of the vertical profile at the well location (1100 meters) of the inverted model using a line search method after 45 iterations. The upper section of the inverted model (between 0 and 500 meters) seems to have the reflectors in their right positions, but the actual velocity values are off. At depths between 1000 and 1200, the reflectors are in their correct depths, but the velocities are off the true values.

In Figure 12, we have plotted the true, starting, inverted velocity using well information, and the inverted velocity models using a line search method away from the well (500 meters). We observe the same trend as in Figures 10 and 11. The inverted model after 45 iterations using well update is better than that from using a line search method.

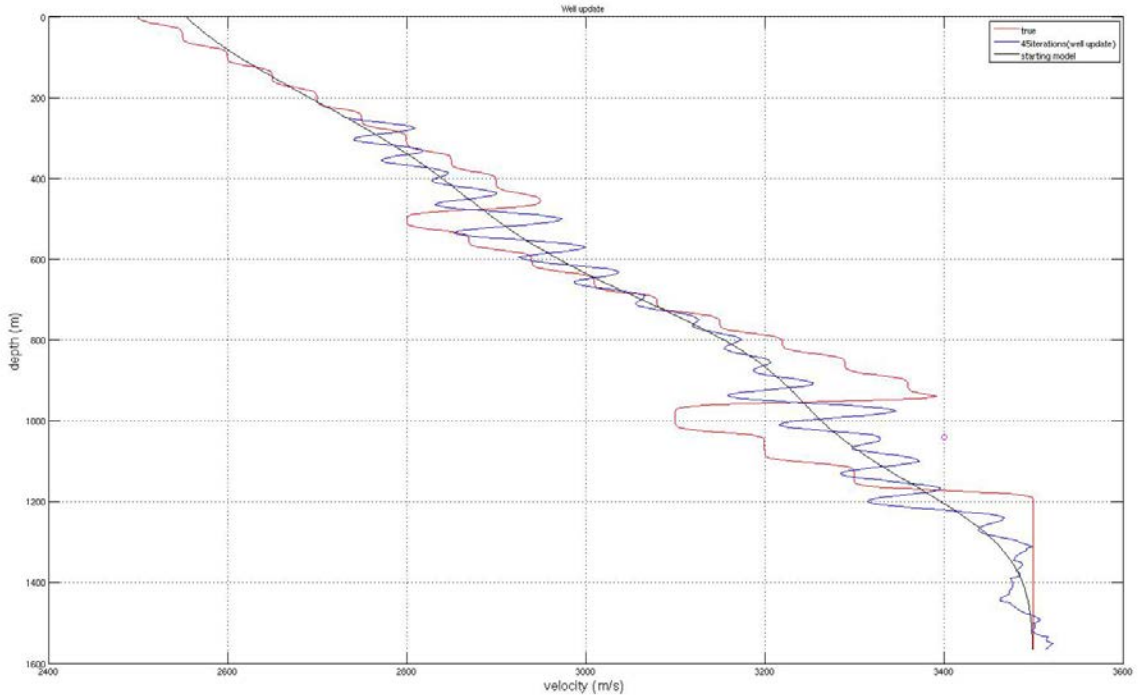

FIG 10. Vertical velocity profile at the well location. True velocity profile (red), smooth velocity profile (black) and inverted velocity profile after 45 iterations using well information (blue).

.

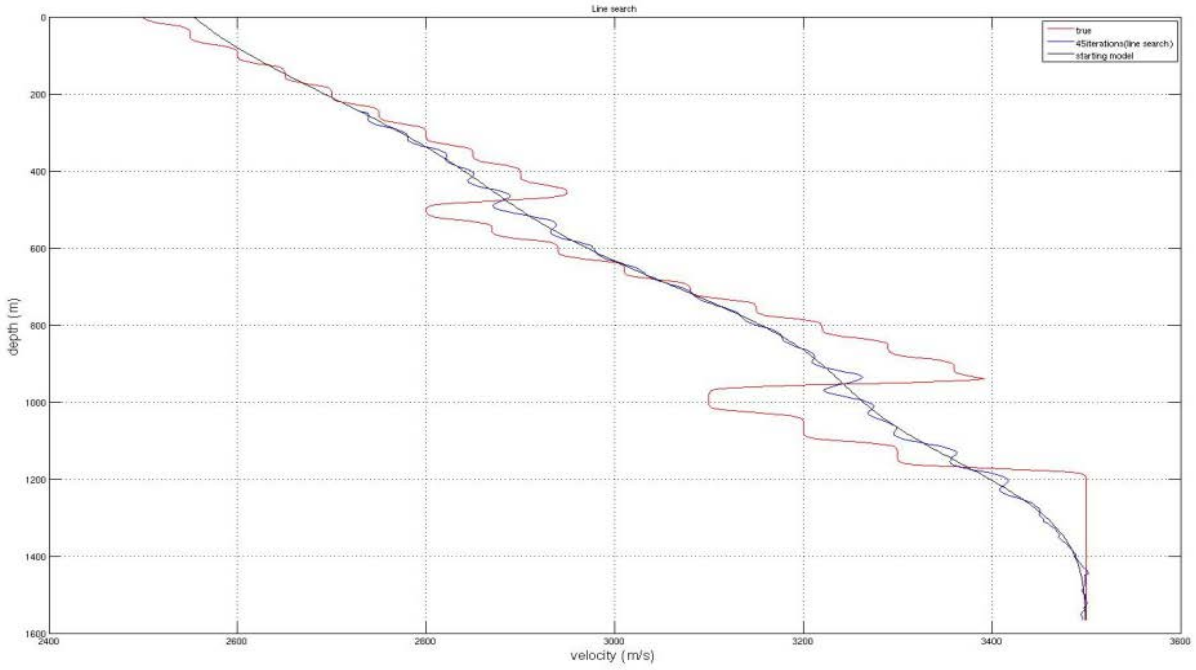

FIG 11. Vertical velocity profile at the well location. True velocity profile (red), smooth velocity profile (black) and inverted velocity profile after 45 iterations using a line search method (blue).

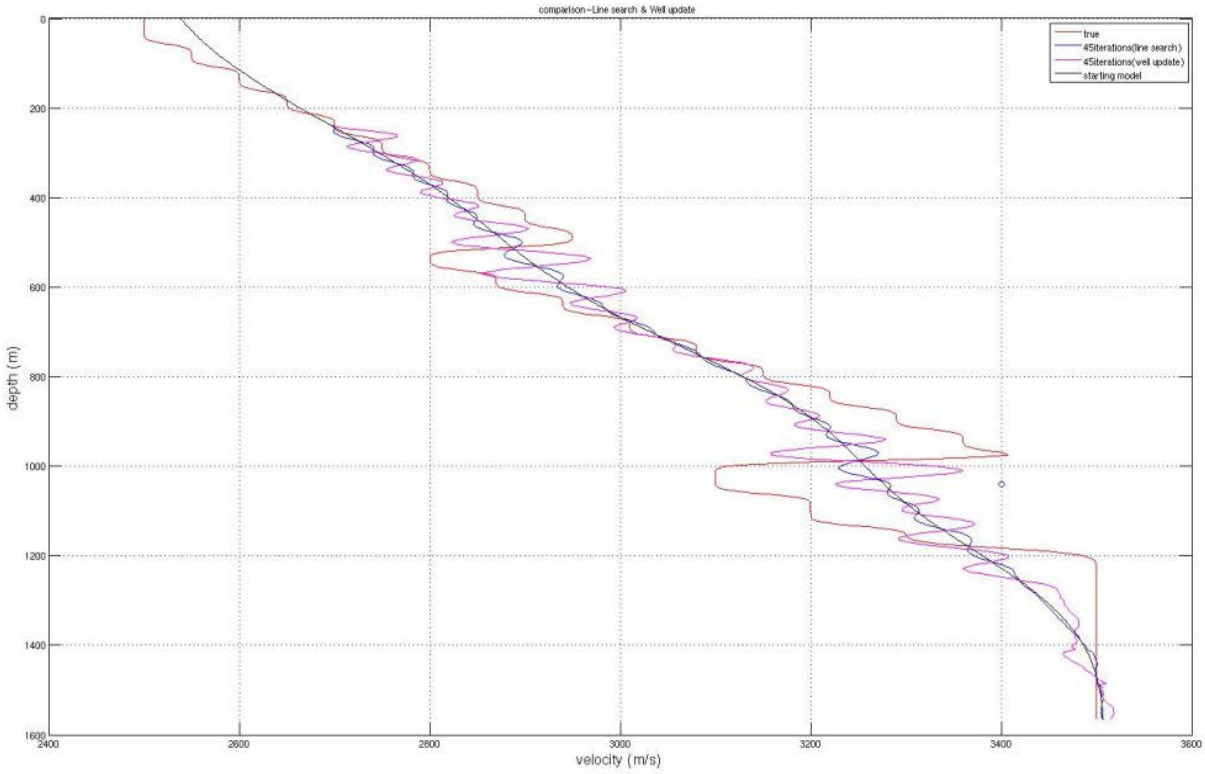

FIG 12. Vertical velocity profile at 500 meters. True velocity profile (red), smooth velocity profile (black), inverted velocity profile after 45 iterations using well information (cyan), and inverted velocity profile after 45 iteration using a line search method (blue).

The best inverted model using a line search method was at the 90th iteration. Beyond the 90th iteration, we did not notice any appreciable change in the inverted model, therefore we stopped at the 90th iteration. Figure 13 shows the final inverted velocity model using a line search method, Figure 14 is the true model and Figure 15 is the final inverted model using well information.

The final inverted velocity model using a line search method has correctly positioned the apex of the intrusion and the thin layers above the intrusion (the region in the boxes in Figure 13) can be seen. The reflectors from the surface down to 500 meters can also be mapped. However the sides of the intrusion cannot be mapped with accuracy.

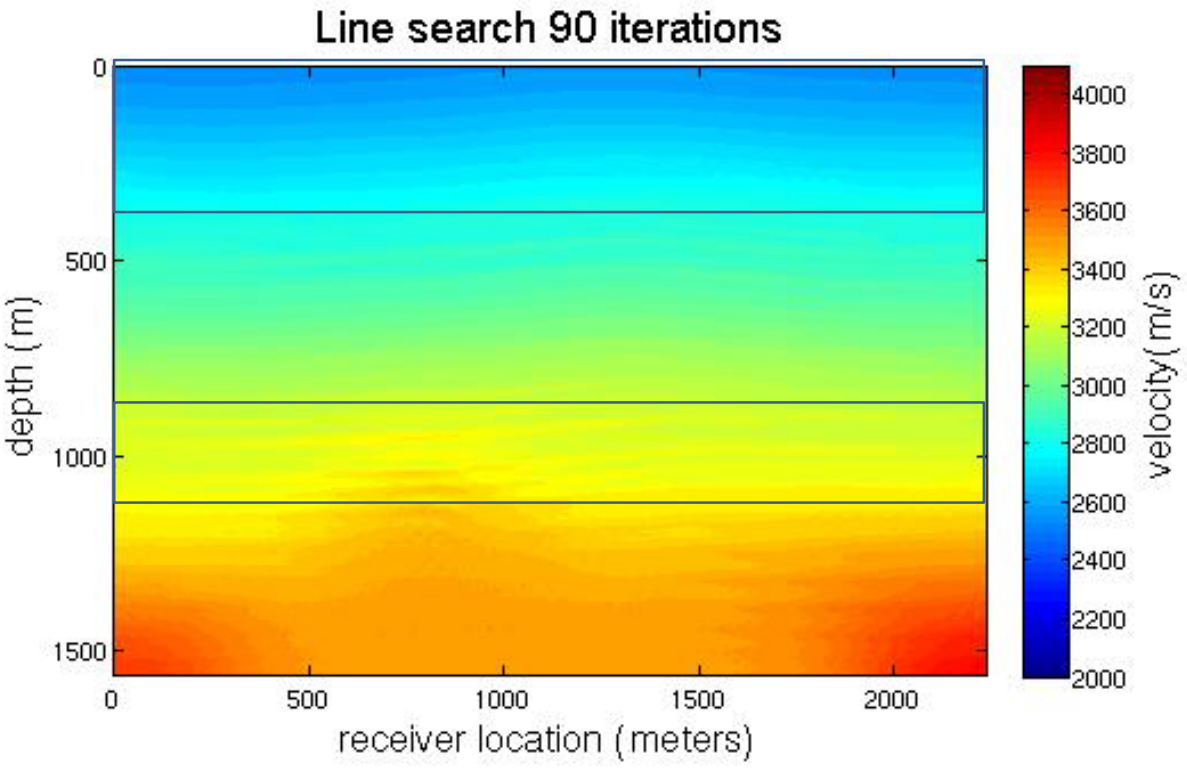

FIG 13. Final inverted velocity model (after 90 iterations) using a line search method. The regions in the boxes show the areas where the reflectors can be easily mapped.

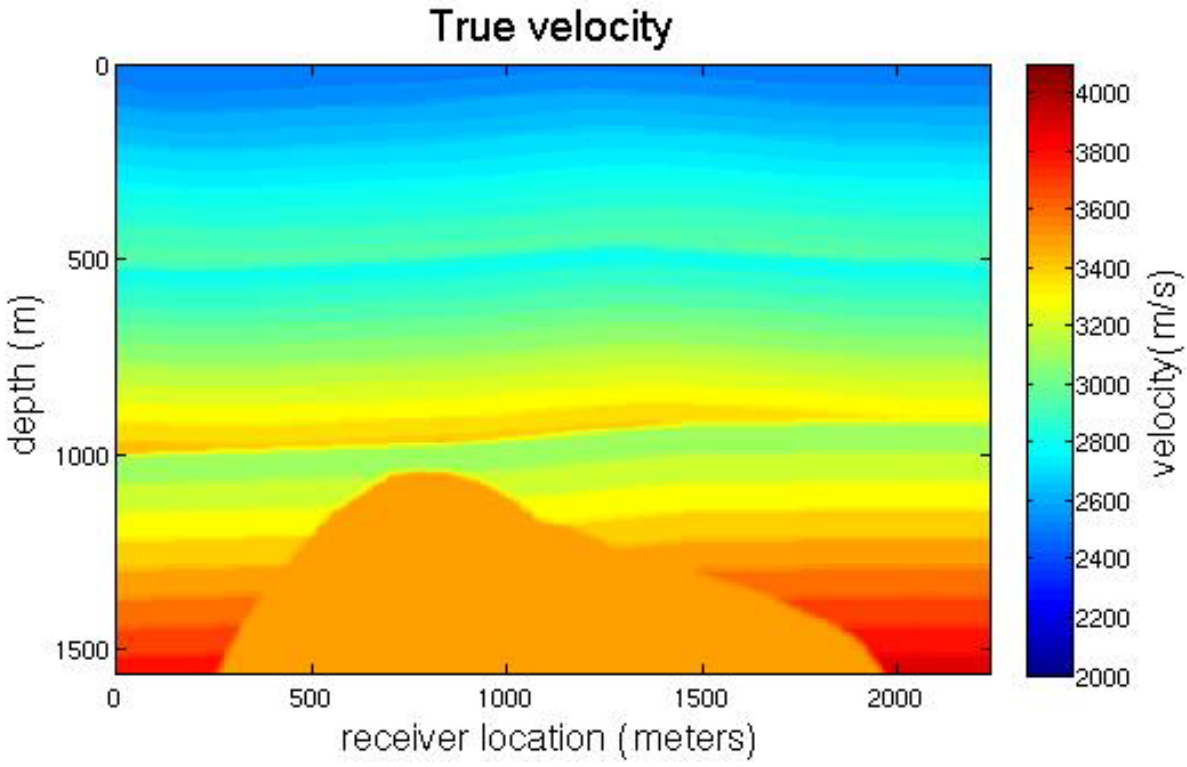

FIG 14.The true velocity model.

From the final inverted model using well information in figure 15, we can map the reflectors below 500 meters (region in the box). The apex of the intrusion appears shallower than it really is, however we can see the sides of the intrusion better than in Figure 13.

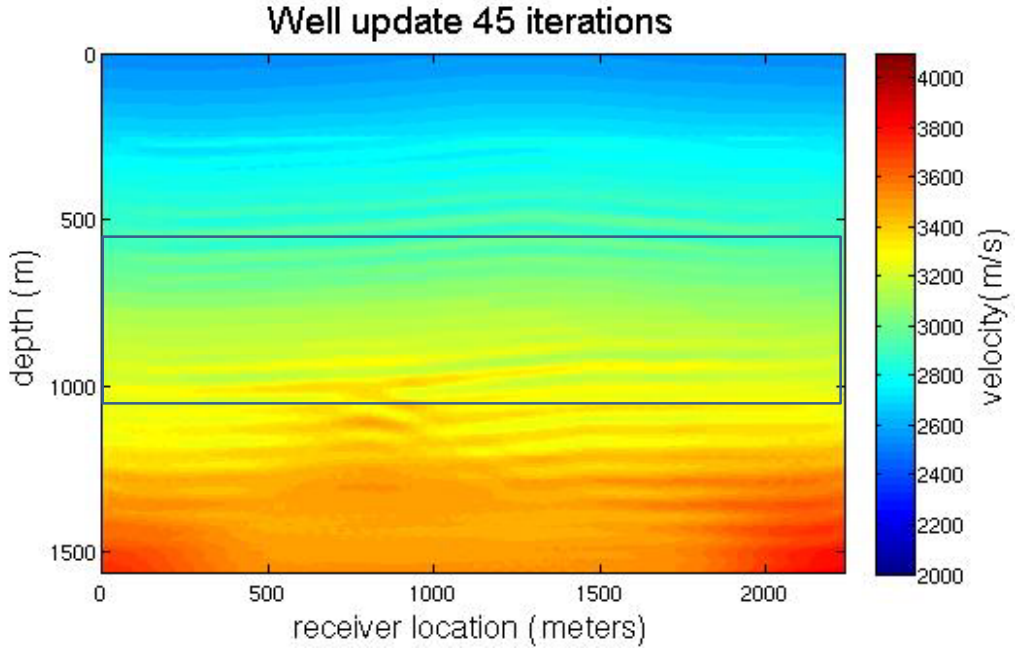

FIG 15. Final inverted velocity model (after 45 iterations) using well information. The region in the box shows the areas where the reflectors can be easily mapped.

Figure 16 is the true velocity model shown again for easy comparison.

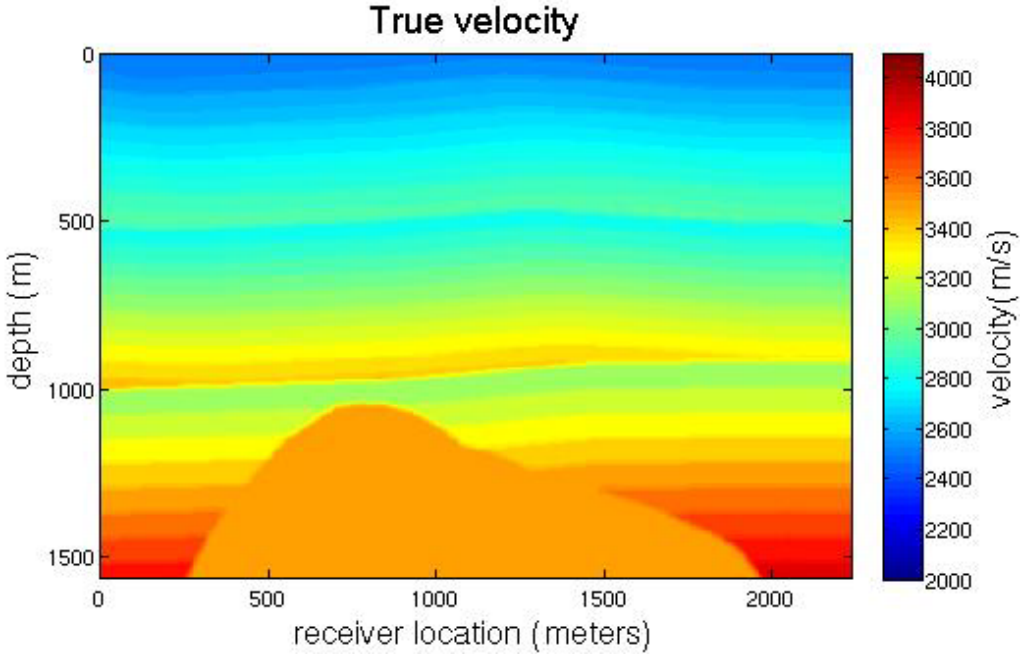

FIG 16. The true velocity model again for easy comparison.

Finally, we compare the path the two methods took to arrive at the 45th iteration in Figures 13 and 15. Figure 17 is a plot of the scalars calculated using Equation 4 and from a line search code.

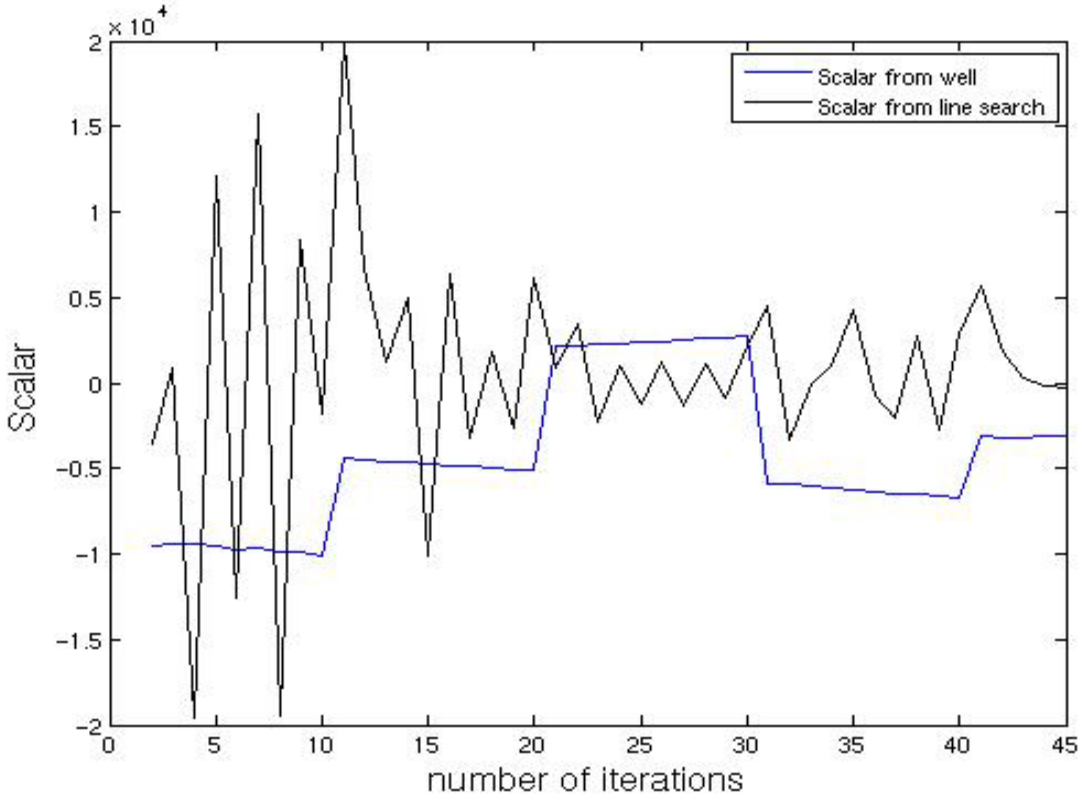

Figure 17. Plot of the scalar from well information (blue), and from a line search code (black), with the scalar computed from the line search code with the value at 1st iteration removed.

In Figure 18 we have plotted the negative of the scalar calculated from well information (red). We see that some of the scalars computed from the line search code lie within the region of plus or minus the value of the scalars calculated using well information.

Similar to the case of the flat layer model, we also observe here that there a few points lie outside this region of plus or minus the value of the scalars calculated using well information. However, we think it is possible to constrain the line search code to search for scalars in the region of plus or minus the calculated scalar from well information. As mentioned earlier, this can save us computational time on the number of forward modelling operations that we would have to run if there is no well information.

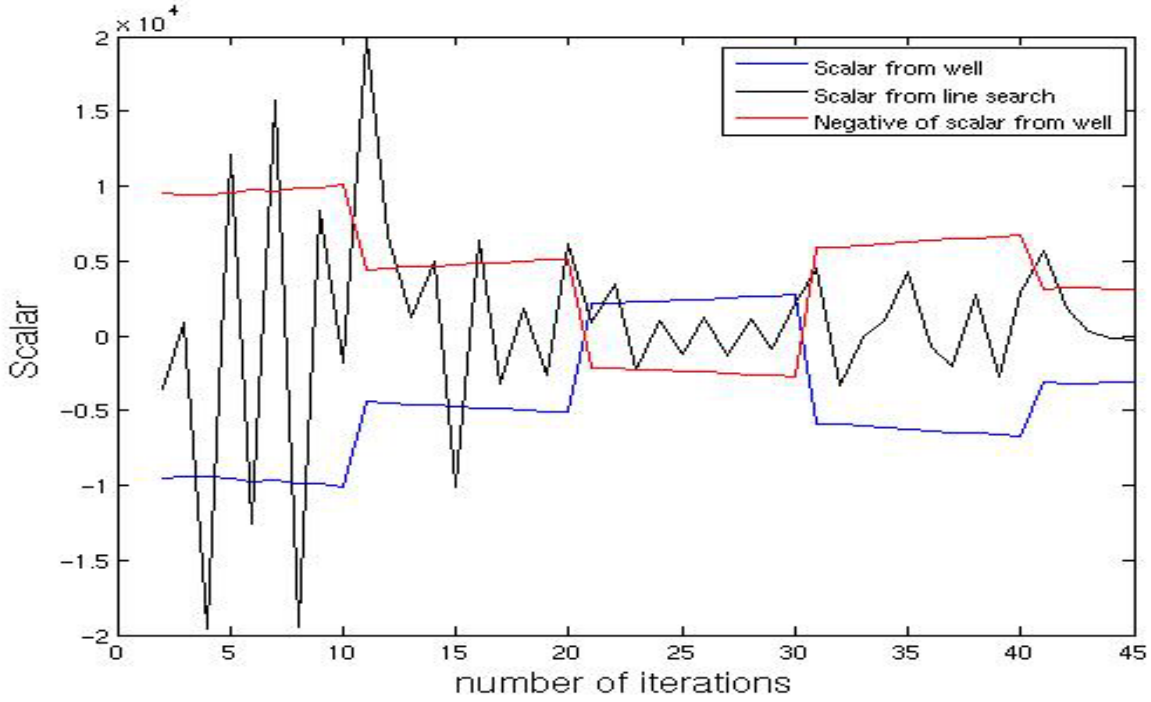

FIG 18. Plot of the scalar: calculated using well information (blue), computed from a line search code (black). The additive inverse of the scalar calculated from well information (red).

Figure 19 is a plot of the vertical velocity profile after 40 iterations using well information. We show this plot here because we believe there is a lot to gain by incorporating well information into FWI. The inverted velocity model after 40 iterations using well update provides a reasonable background trend for the velocity distribution and can be used as a starting model for a line search optimization or other types of optimization method.

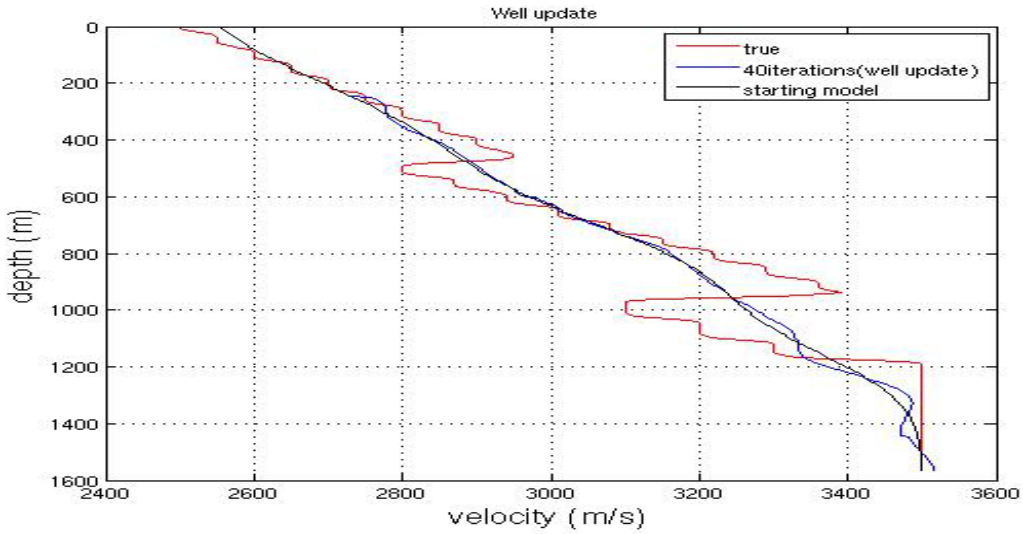

FIG 19. Vertical velocity profile. True velocity profile (red), smooth velocity profile (black), and inverted velocity profile after 40 iterations using well information (blue). The velocity profile can serve as a starting velocity for a line search optimization scheme.

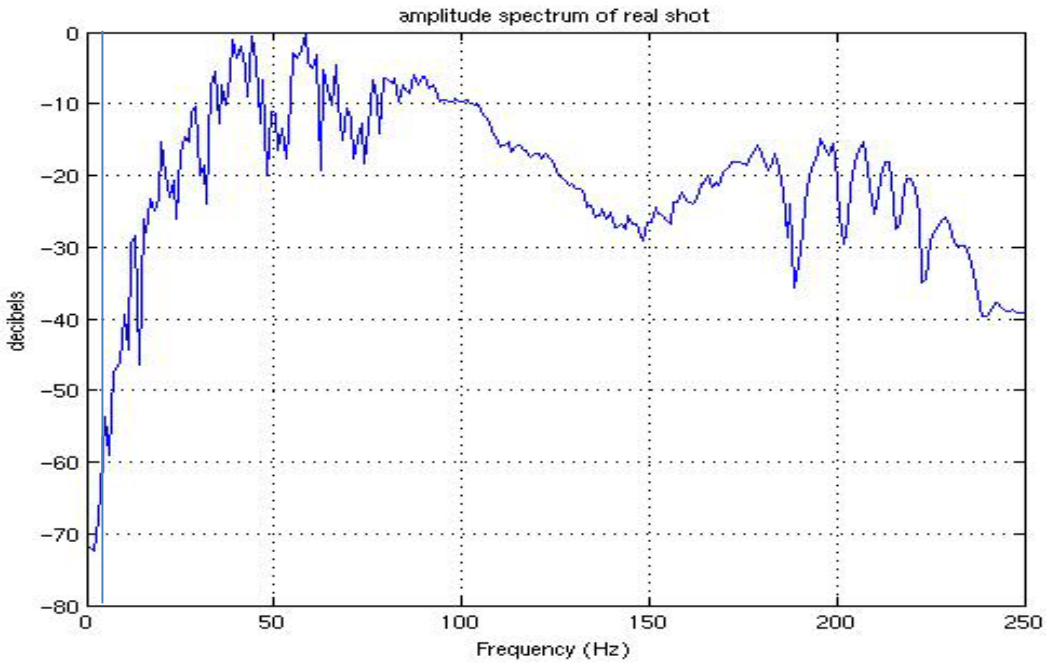

FIG 20. Amplitude spectrum of the first shot. The blue line in the figure corresponds to a frequency of 5 hertz.

DISCUSSIONS AND CONCLUSIONS

In Case 1-a, we were able to show after 50 iterations that using a linear velocity v(z) as a starting model for FWI did not give 'good' results compared with using a smoothed version of the true model as a starting model. We believe this is one of the limitations of conventional FWI. For conventional FWI to produce desirable results, the starting model needs to be close to the true model. The starting model usually can be from traveltime tomography, or Migration Velocity Analysis (MVA). The inverted model after 50 iterations when the starting model was a smoothed version of the true model gave better results.

In Case 1-b, we compared two methods of optimization: using well information to obtain the scalar for the model update and using a line search. We used the exact same starting models in both methods. After 50 iterations, the inverted velocity model using well information produced a better result compared to the inverted model using a line search method as the vertical velocity profiles trough the final models reveal. The reason for this may be due to the fact that we have good well control.

However, the final inverted models are not close to the true model and they converge very slowly which will take several iterations and computational time for convergence. In retrospect, we believe this may be due to the following reasons that are somewhat related:

1. The flat layer model has 3 layers, each layer has a thickness of about 500 meters. The dominant frequency of the wavelet used for modelling is 50hertz, and the average velocity of the 3 layers is 3km/s. If we assume the limit of vertical resolution for stratified layers is one-quarter of the source wavelength, and we work our way backwards to estimate the minimum frequency required to resolve

the thick layers in our model, that is about 1.5 hertz. Analysis of the amplitude spectrum (Figure 20) from our data reveals that we don't have useable low frequencies in our data, even though we began the iteration from 1 hertz. We believe that this is one of the reasons why the flat layer model converges very slowly. Using a wavelet with a dominant frequency of 5 hertz, could produce desirable results with the flat layer model or simply whitening the spectrum before FWI.

2. We feel that the flat-layer model is an oversimplification of a true geological model and of course it is possible to have flat layer geology. However with the bed thickness in our model, it appears the flat layer model represents a 'background' model that can only be resolved by the presence of very low frequencies. We will investigate if better results will come from a model using reflectivity from a well log.

FWI begins at very low frequencies before moving on to higher frequencies. The reason we typically start with the low frequencies is to invert for the background velocity or long wavelengths components of the velocity field. We also begin with very low frequencies in order to avoid cycle skipping problems. Usually moving on to higher frequencies proceeds only after the inversion at lower frequencies have stabilized (Margrave et al, 2010, Pratt 1999). An intuitive way of explaining this as we found in this work is that when running FWI, it is desirable to delay the sharp boundary (reflectors) updates that may leak into the inversion from high frequencies for as long as possible until all the low frequencies have been exploited. This is important because once the sharp boundaries from the high frequencies leak into the inversion, it will be very difficult to remove these boundaries or relocate them to their correct depths. This may also be one of the reasons why users of FWI try to smooth the model in the early parts of the iterations.

Therefore we recommend that early iterations of FWI require as much interaction from the geophysicist. Among other parameters such as the length of the smoother to apply between iterations, the kind of mute to apply to the migrated data residuals, a careful planning of the frequency bands to use in FWI is critical to the success of FWI.

In Case 2, we compared using a line search optimization scheme with incorporating well information by calculating a scalar using Equation 4. We are not making any conclusions about what method works better than the other, as we observed from the results that the line search method resolved the apex of the intrusion, and placed it at the correct depth. However it could not resolve the sides of the intrusion. In addition, the top of the model down to about 500 meters has a better resolution compared with the inverted model using well information.

On the other hand, the inverted model using well information resolved the sides of the intrusion better than the line search method. The reflectors above the intrusion were also resolved, however the apex of the intrusion was not in its correct depth. In Figure 19, we showed that the inverted model after 40 iterations could serve as a starting model to other optimization schemes. In view of this, we conjecture that a combination of a line search

optimization scheme or any other type of optimization scheme with well information should produce desirable results than if only one method of optimization is used.

We also believe that we can use well information to condition the line search code. Figures 8 and 18 show that the scalars computed from the line search code lie between plus or minus the value of the scalars calculated using well information or from Equation 4. This can save a lot of computational time since we can limit the number of forward modelling operations in the line search code. For the size of our model (2235 meters wide by 1565 deep), running 40 shots and 45 iterations using well information took about 15 hours, while for the line search optimization scheme it took 17 hours to run. This might not seem too much of a difference, but with increasing number of shots and for larger models such as a 3D model, the difference might be significant.

Finally, comparing the two models used in this study, we see that we were more successful in our tests using a model with structures than the flat model. In this case, the model with structures, though more complex, is a more realistic earth model than the flat layer model with layer thickness of about 500 when the dominant frequency in the source wavelet is about 50 hertz.

ACKNOWLEDGEMENTS

We thank the sponsors of CREWES for their support. We also gratefully acknowledge support from NSERC (Natural Science and Engineering Research Council of Canada) through the grant CRDPJ 379744-08. We thank Marcelo Guarido for the line search code.

REFERENCES

Biondi, B., Almomin, A., 2012; Tomographic full waveform inversion (TFWI) by combining full waveform inversion with wave equation migration velocity analysis, SEG Technical Program Extended Abstracts, 1-5.

Gazdag, J., and Squazerro, P., 1984, Migration of seismic data by phase shift plus interpolation: Geophysics, 49, 124-131.

Lailly, P., 1983, The seismic inverse problem as a sequence of before stack migrations: Conference on Inverse Scattering, Theory and Application, Society of Industrial and Applied Mathematics, Expanded Abstracts, 206-220.

Margrave, G. F., Ferguson, R. J., and Hogan, C. M., 2010, Full waveform inversion with wave equation migration and well control: in the 22nd Annual Research Report of the CREWES Project.

Margrave, G. F., K. Innanen, and M. Yedlin, 2011a, Full waveform inversion and the inverse Hessian: in the 23nd Annual Research Report of the CREWES Project.

Pratt, R. G., 1999, Seismic waveform inversion in the frequency domain, Part I: Theory and verification in a physical scale model: GEOPHYSICS, 64, 888-901.

Pratt, R.G., Shipp, M., 1999; Seismic waveform inversion in the frequency domain-II: Fault delineation in sediments using crosshole data, Geophysics 64, 901-913.

Tarantola, A., 1984, Inversion of seismic reflection data in the acoustic approximation: GEOPHYSICS, 49, 1259-1256.

Warner, M., Guasch, L., 2014; Adaptive waveform inversion, SEG Technical Program Extended Abstracts, 1089-1093